Determination of the proximity potential from sub-barrier fusion data

M. Inui and S. E. Koonin
W. K. Kellogg Radiation Laboratory, California Institute of Technology, Pasadena, California 91125
(Received 20 December 1983)

Sub-barrier fusion cross sections for 12 systems involving *p*-shell nuclei are analyzed in an attempt to determine directly the universal form of the internucleus potential. We use a previously developed inversion procedure based on the Wentzel-Kramers-Brillouin approximation, which new model calculations presented here show to be highly accurate. The scaling implied by the proximity formulation is found to be roughly consistent with the data, with the structure of the colliding nuclei having little effect. The proximity function Φ determined from the data is consistent with the original function of Blocki *et al.* at intermediate separations, subject to the use of a different formula for the nuclear radii. Data for selected systems involving *sd*-shell nuclei lead to a more attractive potential than that found for the *p*-shell systems, while data for systems involving Ca isotopes exhibit "reentrant" barriers characteristic of a breakdown of the basic assumptions of the inversion procedure.

I. INTRODUCTION

At the simplest level, the low-energy fusion of two large nuclei is governed by penetration of the barrier formed by the repulsive Coulomb and attractive nuclear interactions. Careful measurements and analyses of low energy fusion cross sections might therefore teach us about both the internucleus potential and the tunneling process itself. Such an analysis is the subject of the present paper.

The two elements of sub-barrier fusion, the potential and the tunneling, have broad implications in nuclear physics. The internucleus potential is an essential element in the description of heavy ion collisions of all types at all energies and its systematic properties are a basic feature of nuclear systems. The universal form of this interaction is therefore of interest, both for its application in describing diverse nuclear phenomena and as a background against which to identify possible anomalies, perhaps due to the specific structure of the nuclei involved. The penetration process involved in fusion is that characteristic of a quantum system having many degrees of freedom, a problem which also appears in many other physical situations [e.g., molecules, super-conducting quantum interference devices (SQUIDS)]. The effect of such additional degrees of freedom on the penetration process (i.e., the extent to which the system can be described by a single coordinate) is a subject of considerable interest. In the nuclear case, there have been suggestive model calculations, although a coherent picture is yet to emerge. Moreover, the role of the conventional imaginary part of the optical potential as a description of fusion, in contrast to tunneling through a real potential barrier (perhaps with a few additional degrees of freedom), must also be elucidated.[1]

Our understanding is not yet at the stage where we can simultaneously address all of these questions. Therefore, we will assume in this paper that the tunneling process in sub-barrier fusion is well understood and so seek information about the internucleus potential. One very appealing and general formulation of the nuclear part of this potential relates it to the interaction energy per unit area between two flat surfaces of nuclear matter at a given separation. Such an assumption leads to a proximity potential between any two nuclei of the form[2]

$$V_p = 4\pi\gamma\bar{R}\Phi(\zeta) , \tag{1}$$

where γ is the surface energy coefficient of the semi-empirical mass formula, $\bar{R}$ is the harmonic mean of the central radii of the two nuclei involved (assumed here to be spherical), ζ is the separation of two nuclear surfaces in units of the surface thickness b, and $\Phi(\zeta)$ is the dimensionless universal proximity potential function.

There are basically two types of experimental data whose analyses have been used to determine Φ. Elastic scattering cross sections near the classical rainbow angle have been shown to be sensitive to the extreme tail of the internucleus potential, and a careful analysis by Christensen and Winther has determined Φ for separations $\zeta \gtrsim 2.5$.[3] In a complementary sense, the interaction barrier height and radius extracted from a classical analysis of above-barrier fusion excitation functions have been shown to yield one value of Φ for each system considered.[4] While these data probe smaller separations than do the elastic scattering measurements (spanning the range $\zeta \gtrsim 1.0$), the substantial experimental and theoretical uncertainties involved do not result in a very precise determination of the proximity function.

Recently, it has been demonstrated[5] that sub-barrier fusion excitation functions can be used directly to determine the shape of the interaction barrier as a function of the internucleus separation. The method of analysis, which is summarized briefly below, is based on the Wentzel-Kramers-Brillouin (WKB) approximation and the assumption that fusion is determined by penetration through a real, one-dimensional, energy-independent potential barrier. Within these constraints, tests in several model situations (including those presented in Sec. II) show that the method is very accurate. Furthermore, the few analyses of experimental data for light nuclei present-

ed in Ref. 5 suggest that a systematic study might lead to a determination of the internucleus potential at smaller separations and with smaller uncertainty than has been possible previously.

In this paper, we systematically apply the WKB inversion method to sub-barrier fusion excitation functions for systems involving p-shell nuclei to determine the proximity function Φ. We find that the scaling of the internucleus potential implied by Eq. (1) is valid for many of the systems considered. This is rather surprising in view of the fact that (1) is based on a leptodermous approximation, of questionable validity for light nuclei. In the range $1.5 \lesssim \zeta \lesssim 3.0$, Φ is roughly consistent with the original function in Ref. 2 (exponential in this region), subject to the use of a different formula for the nuclear radii. Furthermore, our results indicate that the structure of the colliding nuclei has little influence on the internucleus potential extracted from the data. That is, apart from the obvious (and still unexplained) structure in $^{12}C + ^{12}C$, it makes no difference whether or not α-conjugate nuclei are involved. (One exception to this statement is the $^{16}O + ^{16}O$ system, discussed in Sec. III.)

We have also analyzed data for the sd-shell systems $^{32,34}S + ^{24,25,26}Mg$ and $^{32}S + ^{27}Al$ (Ref. 31), and for the Ca isotope systems $^{40}Ca + ^{40,44,48}Ca$ (Ref. 32). For S + Mg and S + Al, we find that the scaling of the proximity formalism is again valid, although with a somewhat stronger Φ than that found for the p-shell systems. We also find that although the Ca + Ca systems probe Φ at smaller ζ, they cannot be described by the simple one-dimensional model we use. Rather, these systems require very thin potential barriers with reentrant behavior similar to those found for the even heavier systems discussed in Ref. 5.

The balance of this paper is organized as follows: In Sec. II, we briefly review the WKB inversion method used to determine the internucleus potential directly from the sub-barrier fusion excitation function. Model calculations are also presented here which show that the crucial WKB approximation is highly accurate for the systems of interest. In Secs. III and IV, we present and discuss the results of our analyses of data for 12 p-shell systems, as well as for selected systems involving sd-shell nuclei and the Ca isotopes.

II. METHOD

A method for determining the shape of the interaction barrier between two nuclei from low-energy fusion cross section data is fully explained in Ref. 5. It is semiclassical in nature and is closely related to the RKR method for determining the potentials of diatomic molecules from their vibrational spectra.[6] The method can be summarized by the following equations giving the barrier height, B, and the "thickness" of the barrier, $t(V)$ (the distance between the inner and outer turning points at an energy $V < B$):

$$\left. \frac{d}{dE}\left[\frac{E\sigma}{\pi R^2}\right]\right|_{E=B} = \frac{1}{2} , \tag{2}$$

$$t(V) = -\frac{2}{\pi}\left[\frac{\hbar^2}{2m}\right]^{1/2} \int_V^B \frac{(dS_0/dE)dE}{(E-V)^{1/2}} . \tag{3}$$

Here, E is the center-of-mass bombarding energy, $\sigma(E)$ is the fusion cross section, m is the reduced mass, and $R^2(E)$ characterizes the angular momentum dependence of the penetration coefficient. Following the discussion and results of the model calculations of Ref. 5, we take $R(E)$ to be the average of the barrier radius, R_B, and the Coulomb turning point, $R_C(E) = Z_1 Z_2 e^2/E$; that is,

$$R(E) = \tfrac{1}{2}[R_B + R_C(E)] . \tag{4}$$

Finally, the cross section enters into Eq. (3) through the s-wave action,

$$S_0(E) = \tfrac{1}{2}\ln\left[\left[\frac{d}{dE}\frac{E\sigma}{\pi R^2}\right]^{-1} - 1\right] . \tag{5}$$

Equations (2)—(5) are incomplete in the sense that the barrier radius R_B is not determined from the data, but rather must be specified for each system on some other basis. Furthermore, Eq. (3) gives only the thickness of the interaction barrier, so that to determine the inner turning point (and hence the nuclear potential at small surface separations), we must specify the outer turning point in some way. This latter is relatively straightforward since, for the light systems we consider, the nuclear potential at the outer turning point vanishes very quickly when V becomes even slightly less than B. However, the outer turning point and R_B are related since we require continuity of the potential at the top of the barrier. In our analysis, we have assumed that the outer turning points are determined by the sum of the Coulomb potential for two point charges and an attractive exponential nuclear potential, with the range and strength of the latter adjusted to reproduce the barrier height determined from the data through Eq. (2). We took the barrier radius for each p-shell system to be that obtained from the global potential fitted to elastic scattering data by Akyüz and Winther (AW).[7] For most of the systems considered, this led to a range of the exponential defining the outer part of the barrier in the interval 0.15—0.8 fm (see Table II). Apart from having the advantage of being founded on experiment, these barrier radii are superior to those obtained with the original proximity function of Blocki *et al.*, which generally led to unphysically large exponential ranges of over 1 fm. For consistency, we therefore also used the nuclear radii of Ref. 7,

$$R = (1.20A^{1/3} - 0.35) \text{ fm} , \tag{6}$$

to relate the surface separation to the nuclear separation. For the sd-shell and Ca isotope systems we considered, the AW model often predicts barrier radii which do not agree with those obtained from above-barrier fusion data through the relation

$$\sigma = \pi R_B^2\left[1 - \frac{B}{E}\right] . \tag{7}$$

We therefore used the radii extracted from the above-barrier data in our analysis of these cases. Overall, one should note that our general results and conclusions are relatively insensitive to the choice of R_B, although they do depend upon the choice of Eq. (6) to describe the nuclear radii. In scaling our results to the proximity form

(1), we used a surface thickness $b=1$ fm to relate the surface separation to the dimensionless variable ζ and used the surface energy coefficient γ given by Eq. (28) of Ref. 2.

Equations (3) and (4) show that the barrier thickness is determined by the second derivative of the fusion cross section with respect to energy. This has been obtained from the data by smoothing and interpolating the experimental points with a polynomial in energy fitted to $\ln(E\sigma/\pi R^2)$. In most cases, the order of the polynomial had to be at least 6 for an adequate and stable reproduction of the data. For the integration in Eq. (3), we changed variables from E to $(E-V)^{1/2}$ to eliminate the square-root singularity of the integrand and used Simpson's rule with 20 points; selected tests with 50 points showed no significant differences. Error analysis was handled by the Monte Carlo method of Ref. 5, in which one averages the results of analyzing many sets of pseudodata randomly generated from the experimental cross sections and their errors; both statistical and systematic errors (where given) were accounted for.

Some calculations testing the overall method defined by Eqs. (2)—(5) were presented in Ref. 5. These consisted of generating fusion cross sections corresponding to a model internucleus potential by summing the exact WKB penetration coefficients in all partial waves and then demonstrating that the inversion procedure could accurately recover this potential. While this is certainly a necessary test of the method, it is not sufficient, as it does not address the validity of the basic WKB approximation itself. In order to do so, as well as to assess the reliability of all numerical aspects of our method, we have performed similar tests using cross sections generated from the incoming wave boundary condition model (IWBC) of Ref. 8. In this wave-mechanical description, the boundary condition of purely incoming waves is imposed at a radius interior to the barrier. Statistical errors of 1% and systematic errors of 15% (typical of the better data sets we considered) were assigned to these cross sections at characteristic energy intervals to check the accuracy of the method in a realistic situation. Typical results of the inversion procedure for plausible nuclear potentials of the Woods-Saxon form are shown in Fig. 1; they are quite satisfactory.

In performing these model tests, we found that the order of the polynomial fit to the data had to be at least 6 for satisfactory results (Fig. 1), and that the order actually needed in a given case depended on the barrier radius, on the strength and diffuseness of the nuclear potential, and on the number of cross section points used. It is interesting to note that the order of the polynomial required increases as the diffuseness becomes smaller. The order needed with a diffuseness of 0.5 fm was typically 7 or more. We also found that a precise determination of the barrier height B from Eq. (2) is very important in reducing the uncertainties in the potential extracted. In particular, if a data set does not include cross sections at energies above the barrier, it is impossible to obtain significant results for the nuclear potential. How far the data must extend above the barrier depends upon how well B can be determined; typically, a set with the data 1 MeV above the barrier can gave well-defined results.

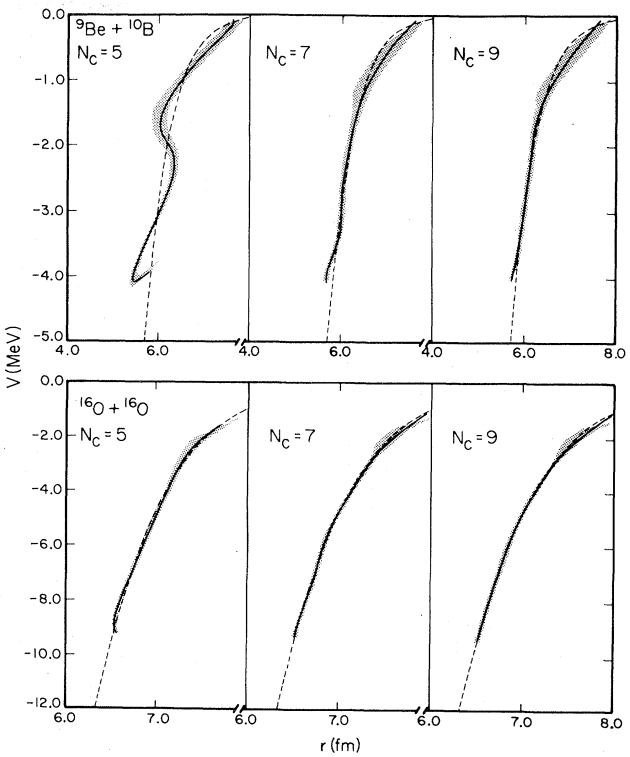

FIG. 1. Results of model calculations testing the inversion algorithm. IWBC cross sections for a Woods-Saxon plus Coulomb potential were inverted to obtain the nuclear potential. Dashed lines indicate the original Woods-Saxon potential, while the solid lines and shaded area indicate the mean and uncertainties of the potential determined by inversion, the uncertainties corresponding to 1% statistical and 15% systematic errors in the pseudodata; N_C is the degree of the polynomial fit used in smoothing and interpolating the pseudodata. The values of R_B used in the inversion were those of the actual potential. Upper: ^{9}Be + ^{10}B, Woods-Saxon parameters $V_0=50.0$ MeV, $R_0=4.61$ fm, $a=0.50$ fm, $R_B=7.21$ fm; lower: ^{16}O + ^{16}O, Woods-Saxon parameters $V_0=50.0$ MeV, $R_0=5.64$ fm, $a=0.60$ fm, $R_B=8.09$ fm.

With these points in mind, we conclude that it is possible to reconstruct the shape of the interaction barrier from the fusion excitation function with satisfactory accuracy. We therefore believe that the systematic application of this method is a dependable way of testing the universal form of the internucleus potential.

III. RESULTS

A. p-shell systems

We have considered over 22 data sets for 15 p-shell systems in an effort to determine the proximity potential using the method explained above. These data sets are listed in Table I. (We also include ^{12}C + ^{20}Ne since the mass of the compound system is comparable to that for the other systems considered.) As in any analysis attempting to extract global features from experimental data, our task is

TABLE I. Data used for systems involving p-shell nuclei.

System	Ref.	Fitted	Remark
$^{9}Be + {}^{10}B$	10		Anomalously large cross sections
$^{10}B + {}^{10}B$	11		No data above barrier
$^{9}Be + {}^{12}C$	12		Anomalously large cross sections
$^{10}B + {}^{11}B$	11		No data above barrier
$^{10}B + {}^{12}C$	13		No data above barrier
$^{10}B + {}^{12}C$	14	×	
$^{11}B + {}^{11}B$	11		No data above barrier
$^{11}B + {}^{12}C$	13		Data too imprecise
$^{11}B + {}^{12}C$	14	×	
$^{10}B + {}^{14}N$	13		No data above barrier
$^{10}B + {}^{14}N$	15	×	
$^{12}C + {}^{12}C$	16		Resonances
$^{12}C + {}^{12}C$	17		Resonances
$^{12}C + {}^{12}C$	18		Resonances
$^{9}Be + {}^{16}O$	19		Anomalously large cross sections
$^{12}C + {}^{13}C$	20	×	
$^{12}C + {}^{14}N$	21	×	
$^{13}C + {}^{13}C$	22	×	
$^{13}C + {}^{13}C$	23		Less precise than the data above
$^{12}C + {}^{16}O$	24	×	
$^{12}C + {}^{16}O$	25		Smaller energy range than the data above
$^{14}N + {}^{14}N$	26	×	No data below 5.8 MeV were used for fit
$^{13}C + {}^{16}O$	27	×	
$^{14}N + {}^{16}O$	21	×	
$^{12}C + {}^{20}Ne$	28	×	No data below 7.0 MeV were used for fit
$^{16}O + {}^{16}O$	29	×	
$^{16}O + {}^{16}O$	28		Similar to the data above
$^{16}O + {}^{16}O$	30		Similar to the data above

complicated by inaccurate or imprecise measurements, and, more interestingly, by any true deviations from systematic behavior. Therefore, in our determination of the proximity function, we have avoided fitting obviously spurious data or data which are too imprecise to be useful. Data sets in the latter category were mostly those which do not have measurements extending sufficiently far above the barrier, as explained at the end of Sec. II; these are indicated in Table I. Data sets in the former category include those for systems involving a ^{9}Be nucleus (where the weakly bound neutron makes the cross sections anomalously high) and those for $^{14}N + {}^{14}N$ and $^{12}C + {}^{20}Ne$ at low energies (below $E \approx 5.8$ and 7.0 MeV, respectively), where large cross sections measured cause the radii determined for the inner turning points to actually increase as V decreases (similar to the reentrant barriers found for much heavier systems in the analysis of Ref. 5). We have therefore not used these data in determining the proximity function, nor have we used any of the $^{12}C + {}^{12}C$ data, whose oscillations clearly cannot be reproduced by any simple barrier penetration model. There may well be interesting physics in these anomalies, but such data are clearly inappropriate for our global analysis. For systems where there are more than one set of data, we have used those measurements which gave the most physically plausible barriers, or those which extended to the smallest energies below B.

The results of our analysis of the remaining 12 systems is summarized in Fig. 2. The uncertainties in the values of ζ determined are typically ≈ 0.1 at $\zeta \approx 2.4$ and ≈ 0.2 at

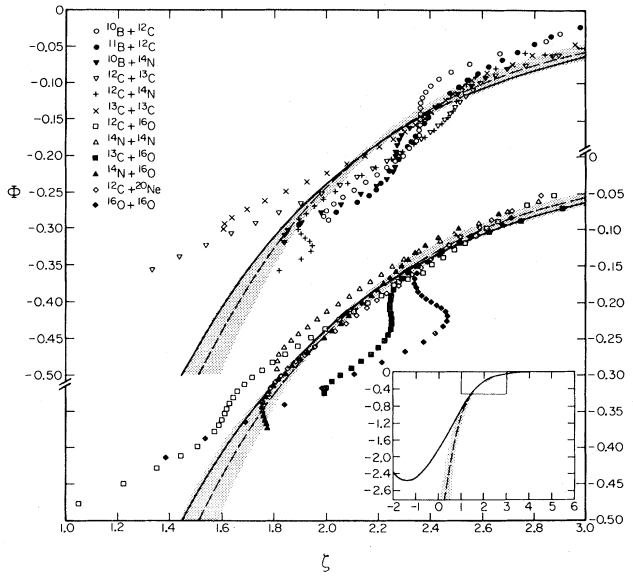

FIG. 2. Proximity function Φ determined from the analysis of p-shell systems. Symbols correspond to potentials obtained by inverting sub-barrier fusion cross sections for the systems indicated; the systems are shown in two separate plots for greater clarity. The dashed line and shaded region indicate the mean and uncertainties in the best-fit exponential function, Eqs. (8) and (9), for all of the systems, while the solid line is the original function of Ref. 2. The inset shows the region covered by the present data in a more global perspective.

TABLE II. Potential barrier parameters.

System	R_B (fm)	B (MeV)	V_0 (MeV)	α (fm)
$^{10}B + ^{12}C$	7.74	5.32±0.11	0.27	0.37
$^{11}B + ^{12}C$	7.86	5.39±0.14	0.11	0.16
$^{10}B + ^{14}N$	7.84	5.80±0.09	0.64	0.77
$^{12}C + ^{13}C$	7.96	5.87±0.09	0.64	0.79
$^{12}C + ^{14}N$	7.95	7.00±0.10	0.61	0.64
$^{13}C + ^{13}C$	8.07	6.01±0.14	0.42	0.52
$^{12}C + ^{16}O$	8.05	7.97±0.06	0.63	0.59
$^{14}N + ^{14}N$	8.06	7.97±0.06	0.54	0.49
$^{13}C + ^{16}O$	8.39	8.23±0.41	0.61	0.62
$^{14}N + ^{16}O$	8.15	9.08±0.05	0.82	0.67
$^{12}C + ^{20}Ne$	8.21	9.84±0.22	0.69	0.54
$^{16}O + ^{16}O$	8.24	10.17±0.17	1.02	0.75
$^{24}Mg + ^{32}S$	9.17	28.00±0.09	2.16	0.67
$^{25}Mg + ^{32}S$	9.19	27.61±0.19	2.50	0.76
$^{26}Mg + ^{32}S$	8.89	27.09±0.09	4.05	1.16
$^{24}Mg + ^{34}S$	9.15	27.42±0.18	2.82	0.85
$^{25}Mg + ^{34}S$	8.86	27.05±0.07	4.18	1.19
$^{27}Al + ^{32}S$	9.04	29.68±0.10	3.47	0.95
$^{26}Mg + ^{34}S$	9.51	27.06±0.13	2.02	0.66
$^{40}Ca + ^{40}Ca$	8.96	52.89±0.08	11.43	1.59
$^{40}Ca + ^{44}Ca$	8.49	52.35±0.19	15.54	1.94
$^{40}Ca + ^{48}Ca$	8.56	52.12±0.22	15.24	1.94

the limits of the data. As explained in Sec. II, we have described the outer turning points by the sum of the Coulomb potential and an exponentially decreasing nuclear potential. The parameters found for these exponential nuclear potentials of the form $-V_0\exp[-(r-R_B)/\alpha]$ are given in Table II, together with the barrier heights obtained from the data through Eq. (2). For most of the p-shell systems, the AW potential gives reasonable barrier radii; a comparison with radii extracted from above-barrier fusion data (Ref. 9) shows that the differences are roughly 0.1 fm or less. Exceptions were the very light systems, $^{10,11}B + ^{12}C$, for which the AW barrier radii were roughly 0.3 fm larger. The barrier radius for $^{13}C + ^{16}O$ was increased by 0.24 fm to compensate for the exceptionally thick barrier near its peak implied by the data.

In view of the uncertainties mentioned above, Figs. 2 and 3 (the latter giving a more global perspective) show a rough validity of the proximity scaling for many p-shell systems, although the limited range of nuclei covered in the data does not allow a particularly stringent test of this scaling. Indeed, it is rather surprising that the proximity formalism, which is based on a leptodermous approximation, gives sensible results when applied to such light nuclei. In this respect, our results demonstrate a rough universality, but should not be construed as "proving" the proximity ideas, as it is likely that a different sort of scaling would yield equally good results.

As there is the rough consistency with the exponential part of the proximity function of Ref. 2, we have chosen to represent the data in the form

$$\Phi_F=\Phi_0\exp[-(\zeta-\zeta_0)/\alpha]\ . \tag{8}$$

Here, we have referred ζ to $\zeta_0=2.0724$, a point at the center of the range we consider, in order that the uncertainties quoted in Φ_0 be meaningful. A least-squares fit to the data results in

$$\Phi_0=0.2195\pm0.0032;\quad \alpha=0.680\pm0.079\ . \tag{9}$$

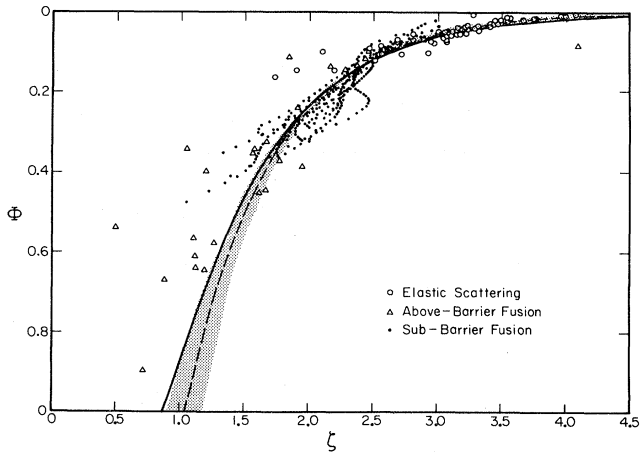

FIG. 3. Values of the proximity function Φ determined from p-shell sub-barrier fusion data, as in Fig. 2, compared with the values determined from elastic scattering (Ref. 3) and from fusion cross sections above the barrier (Ref. 4). The dashed line, shaded region, and solid line have the same meaning as in Fig. 2.

The strength of this function is consistent with the original calculations of Blocki *et al.*, although the smaller diffuseness found in the intermediate region considered here suggests stronger potentials at smaller separations. Note that smaller values of ζ are explored here than are obtained from elastic scattering data, as seen in the inset of Fig. 2 and in Fig. 3. However, the general trend of our results is consistent with the extrapolation of the elastic scattering values and with the above-barrier fusion points, as is shown in Fig. 3. It should also be noted that the sums of the nuclear radii based on Eq. (7) are 0.50—0.55 fm larger than those proposed in the original proximity formulation of Ref. 2, although they are consistent with the values obtained from electron scattering.

Figure 2 shows no great anomalies which might be attributed to nuclear structure, except for $^{16}O + ^{16}O$ (see below). However, the potentials for systems involving one excess neutron, namely $^{11}B + ^{12}C$ and $^{13}C + ^{16}O$, are stronger than average; this is consistent with the very strong potential we would have obtained for the systems involving a ^{9}Be nucleus. Thus, the ability to excite or transfer valence nucleons during the fusion process seems to be important in some cases. All three data sets for $^{16}O + ^{16}O$ gave similar reentrant barriers, corresponding to the "hook" in Fig. 2. Other apparent deviations from the general trend are largely due to an imperfect polynomial fit and to uncertainties of the data; in most cases, they are well within the errors.

Our methods make very stringent demands of the experimental data, as Eqs. (2)—(5) show that the second energy derivative of the fusion cross section is required. Moreover, Eq. (3) shows that the cross section at a given energy influences the thickness of the barrier determined at all lower energies. Hence, small features in the data, whether experimental or perhaps indicative of true weak structure, become important and can have a dramatic influence on our results. One such example is seen in the $^{16}O + ^{16}O$ data shown in Fig. 2, where the hook near $\zeta = 2.4$ depresses the proximity function determined for all smaller separations. As this hook is present in all three data sets we have considered (Refs. 28, 29, and 30), it is possibly a signature of the breakdown of the basic assumptions of our method. Further measurements would be useful to clarify this point, particularly since the evaporation calculations used to relate photon yields to fusion cross sections are suspect.[31] In the same way, a barrier which is unusually thick near its top, as can result from poor experimental data, affects the thickness determined at lower energies. If the experimental cross sections are too small near $E = B$, the barrier will be unreasonably thick near its peak, and so result in a smaller thickness (stronger nuclear potential) at lower energies (smaller separations). Such a barrier, of course, does not represent the actual potential which we are seeking. This seemed to be the case for some of the data sets we considered, which gave strong values for Φ relative to other systems.

With the fitted proximity function Φ_F obtained above, we can reconstruct an internucleus potential barrier for any pair of *p*-shell nuclei. A few examples of barriers found with Φ_F, the AW potential, and from the fusion data are shown in Fig. 4. The barrier heights from Φ_F are

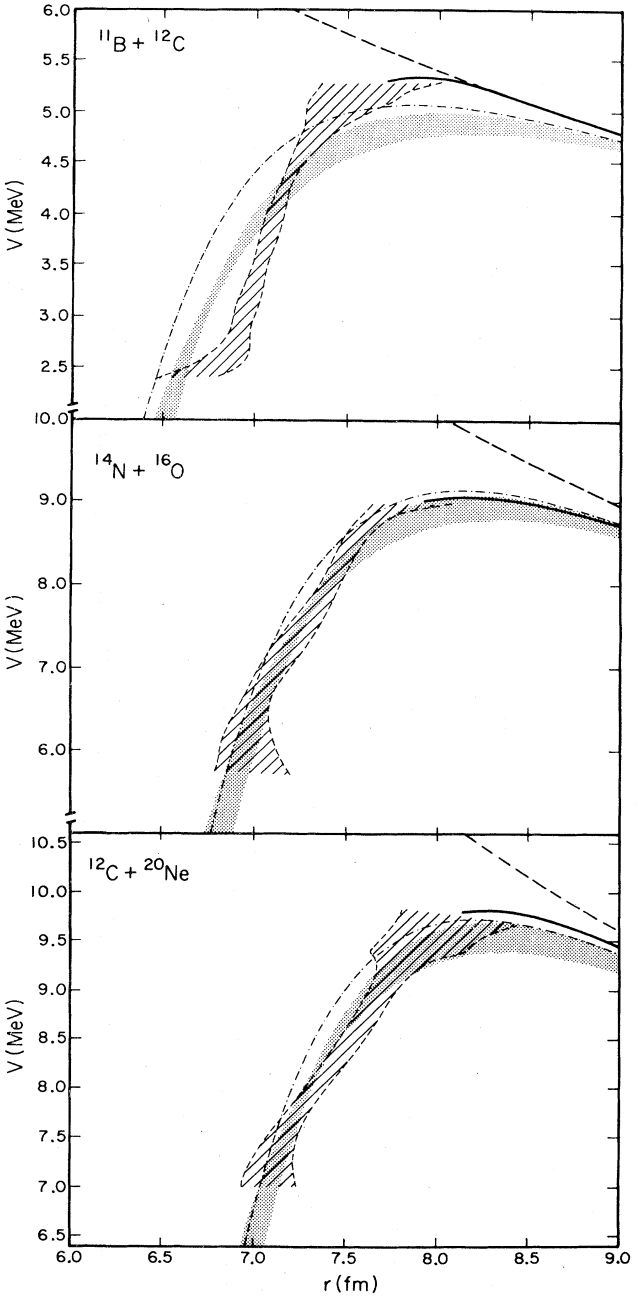

FIG. 4. Barrier shapes determined for several *p*-shell systems. Cross-hatched region and solid line: inner and outer turning points determined by inversion of sub-barrier data; shaded region: barrier determined from global exponential fit, Eqs. (8) and (9); —·—·—·, AW potential; — — —, Coulomb potential for two point charges.

somewhat smaller than those obtained with the AW potential, but they are satisfactorily close to the actual barriers. It is also interesting to note that Φ_F gives an excellent barrier for the system $^{12}C + ^{20}Ne$ even though ^{20}Ne is not a *p*-shell nucleus.

B. *sd*-shell and Ca isotope systems

We have also analyzed data for the systems $^{32,34}S + ^{24,25,26}Mg$, $^{32,34}S + ^{27}Al$ (Ref. 32), and

$^{40}Ca + {}^{40,44,48}Ca$ (Ref. 33). As mentioned in Sec. II, for these systems we determined the barrier radii from the above-barrier data and the well-known relation Eq. (7). In doing so, we took advantage of the very weak dependence of B on R_B as obtained from sub-barrier data through Eq. (2). For example, for the $^{40}Ca + {}^{40}Ca$ data, Eq. (2) gives $B=53.02$ and 52.89 MeV for barrier radii $R_B=9.81$ and 8.96 fm, respectively. Thus, it was possible, with a plausible value of R_B, to determine B quite accurately from the sub-barrier data. The barrier heights obtained in this manner could then be used in Eq. (7) to determine R_B from the above-barrier data. In this way, we could greatly reduce the error involved in determining R_B.

With the radii so defined, we found that the barriers of the systems $^{32,34}S + {}^{24,25,26}Mg$ and $^{32}S + {}^{27}Al$ are physically reasonable (except for $^{24}Mg + {}^{32}S$, which showed a reentrant barrier) and seem to indicate stronger potentials than those expected from the p-shell proximity function, Eqs. (8) and (9), as seen in Figs. 5 and 6. (The uncertainties in our results are similar to those for the p-shell systems discussed above.) This conclusion is subject to the same caveats discussed in connection with the p-shell systems. It is also contingent upon the validity of (6) for the nuclear radii; a systematic underestimate of the radius of each nucleus by 0.1 fm would result in agreement with the p-shell data.

For the systems $^{40}Ca + {}^{40,44,48}Ca$, the results are puzzling, particularly for $^{40}Ca + {}^{44,48}Ca$ (see Fig. 7). The $^{40}Ca + {}^{40}Ca$ barrier is marginally plausible, and results in a proximity function consistent with the p-shell data, although at a much smaller separation, while the $^{40}Ca + {}^{44}Ca$ barrier is clearly unphysical. The cross sections for these systems are much too large at low energies, requiring a very thin barrier. These large cross sections might be due to the dynamic influence of the additional neutron degrees of freedom on the fusion process, which makes the approximations we employ inappropriate. Moreover, the determination of the barrier radii from above-barrier data for these systems was complicated by the inconsistency of Eq. (7) with the data, so that R_B could not be determined with good precision.

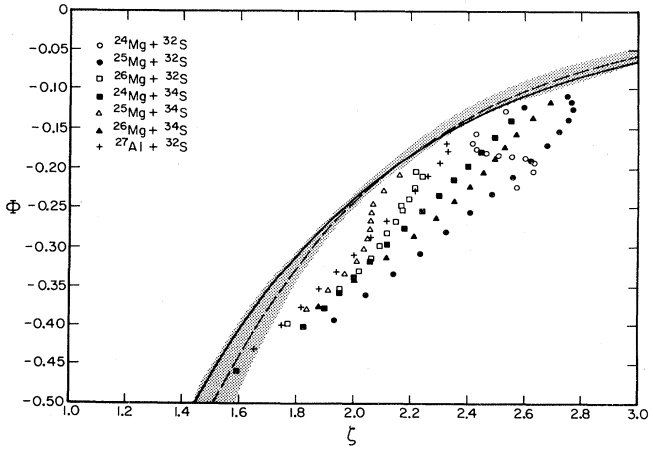

FIG. 5. Similar to Fig. 2 for systems involving *sd*-shell nuclei.

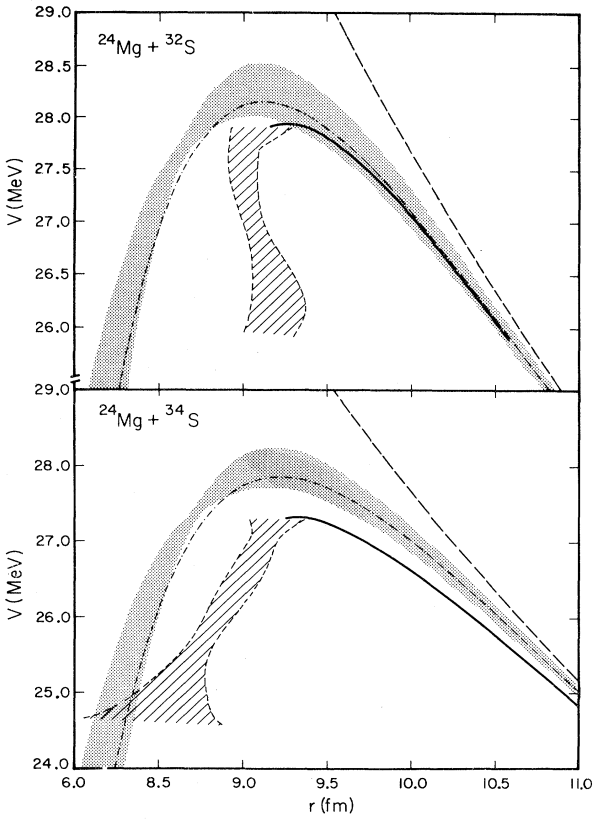

FIG. 6. Similar to Fig. 4 for the $^{24}Mg + {}^{32}S$ and $^{24}Mg + {}^{34}S$ systems.

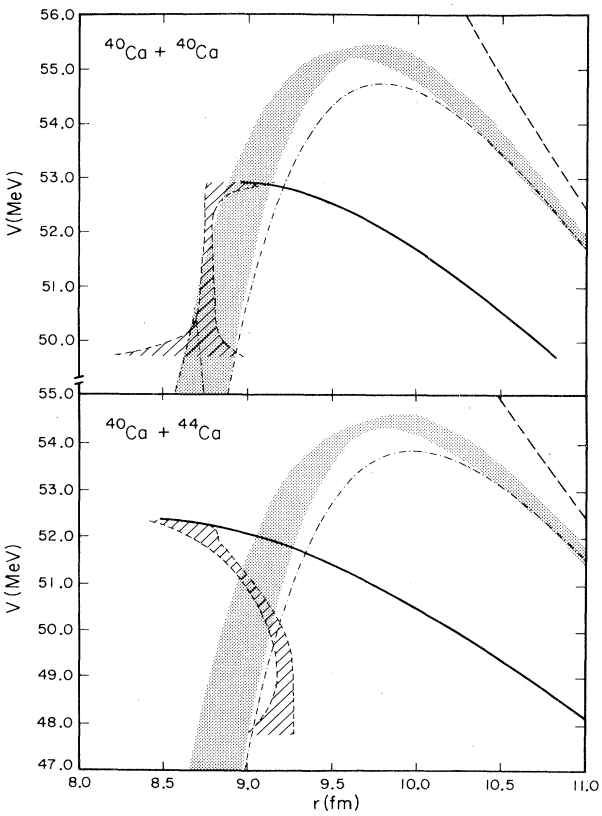

FIG. 7. Similar to Fig. 4 for the $^{40}Ca + {}^{40}Ca$ and $^{40}Ca + {}^{44}Ca$ systems.

IV. DISCUSSION

In this paper, we have employed a previously-developed method of reconstructing internucleus potential barriers from sub-barrier fusion cross sections. Its basic assumption is that fusion is determined by penetration through an energy- and angular-momentum-independent local potential barrier. The tests we have presented in Sec. II demonstrate that the semiclassical nature of the method is appropriate for the systems being considered, if the basic assumption is valid, and that model potential barriers can be reconstructed with high precision.

We have applied this method to fusion data for 12 systems involving *p*-shell nuclei to determine the nuclear interaction at intermediate surface separations. Although there is some scatter in the results, we find that the potentials so obtained roughly obey a proximity scaling with an exponential proximity function and that they probe smaller surface separations than do elastic scattering data. The proximity function we determine is consistent with that obtained from an analysis of elastic scattering data, but is somewhat more attractive than the original of Blocki *et al.* An exponential parametrization of the proximity function reproduces satisfactorily most of the potential barriers obtained from the fusion cross sections. Apart from the obvious oscillations in $^{12}C + ^{12}C$, the structure of the *p*-shell nuclei involved did not have a significant effect on the potential extracted, with the exception of the large cross sections for systems involving a weakly-bound excess neutron and a mysterious hook in the nuclear potential extracted from the $^{16}O + ^{16}O$ data.

For the *sd*-shell systems $^{32,34}S + ^{24,25,26}Mg$ and $^{32}S + ^{27}Al$, we found that the proximity formalism is roughly valid, although the potentials extracted are somewhat stronger than would be predicted from the *p*-shell proximity function. For systems involving the Ca isotopes, $^{40}Ca + ^{40,44,48}Ca$, there is a dramatic influence of the neutron excess on the barriers determined.

On the experimental side, one clear conclusion of our studies is that there is a need for more precise and systematic data, both somewhat above and far below the barrier. Inconsistent measurements of several systems and incomplete energy coverage of others have hampered our attempts to extract universal features of the internucleus interaction. Moreover, our work should motivate measurements to as low an energy as is possible, since fusion cross sections at lower energies yield information about the internucleus interaction at smaller separations.

On the theoretical side, it is necessary to further explore the validity of the basic assumption that fusion is governed by penetration through a real one-dimensional potential barrier and to identify and treat any intrinsic degrees of freedom important in the fusion process. This latter is unlikely to be easy, although the importance of other degrees of freedom might be demonstrated in systems with loosely-bound valence nucleons or deformed nuclei. The fusion cross section is only a single function of energy, and so contains limited information. However, the simultaneous consideration of fusion, transfer, inelastic, and elastic excitation functions in a single system, together with realistic coupled-channels calculations, is an obvious goal to pursue.

ACKNOWLEDGMENTS

M. Inui gratefully acknowledges support by a California Institute of Technology Summer Undergraduate Research Fellowship during much of this work. We thank many of our colleagues in the Kellogg Radiation Laboratory and M. Beckerman and S.-C. Wu for discussions of experimental aspects. We are grateful to P. Braun-Munzinger for sending us data prior to publication. This work was supported in part by the National Science Foundation, Grants PHY82-17332 and PHY83-15500.

[1]W. S. Freeman *et al.*, Phys. Rev. Lett. **50**, 1563 (1983).
[2]J. Blocki, J. Randrup, W. J. Swiatecki, and C. F. Tsang, Ann. Phys. (N.Y.) **105**, 427 (1977).
[3]P. R. Christensen and A. Winther, Phys. Lett. **65B**, 19 (1976).
[4]J. R. Birkelund and J. R. Huizenga, Phys. Rev. C **17**, 126 (1978).
[5]A. B. Balantekin, S. E. Koonin, and J. W. Negele, Phys. Rev. C **28**, 1565 (1983).
[6]A. L. G. Rees, Proc. Phys. Soc., London **59**, 998 (1947); E. A. Mason and L. Mochick, Adv. Chem. Phys. **12**, 329 (1967).
[7]Ö. Akyüz and A. Winther, in *Proceedings of the Enrico Fermi International School of Physics, 1979,* edited by R. A. Broglia, C. H. Dasso, and R. Ricci (North-Holland, Amsterdam, 1980), p. 492; R. A. Broglia and A. Winther, *Heavy Ion Reactions* (Benjamin/Cummings, Reading, Mass., 1981), pp. 108–115.
[8]G. H. Rawitscher, Nucl. Phys. **85**, 337 (1963).
[9]L. C. Vaz, J. M. Alexander, and G. R. Satchler, Phys. Rep. **69**, 373 (1981).
[10]M. L. Chatterjee, H. C. Cheung, and B. Cujec, Nucl. Phys. **A323**, 461 (1979).
[11]M. D. High and B. Cujec, Nucl. Phys. **A259**, 513 (1976).
[12]H. C. Cheung, M. D. High, and B. Cujec, Nucl. Phys. **A296**, 333 (1978).
[13]M. D. High and B. Cujec, Nucl. Phys. **A278**, 149 (1977).
[14]R. A. Dayras, R. G. Stokstad, Z. E. Switkowski, and R. M. Wieland, Nucl. Phys. **A261**, 478 (1976).
[15]S.-C. Wu, J. C. Overley, C. A. Barnes, and Z. E. Switkowski, Nucl. Phys. **A312**, 177 (1978).
[16]M. D. High and B. Cujec, Nucl. Phys. **A282**, 181 (1977).
[17]M. G. Mazarakis and W. E. Stephens, Phys. Rev. C **7**, 1280 (1973).
[18]J. R. Patterson, H. Winkler, and C. S. Zaidins, Astrophys. J. **157**, 367 (1969).
[19]Z. E. Switkowski, S.-C. Wu, J. C. Overley, and C. A. Barnes, Nucl. Phys. **A289**, 236 (1977).
[20]R. A. Dayras, R. G. Stokstad, Z. E. Switkowski, and R. M. Wieland, Nucl. Phys. **A265**, 153 (1976).
[21]Z. E. Switkowski, R. G. Stokstad, and R. M. Wieland, Nucl. Phys. **A279**, 502 (1977).
[22]S. Trentalange, Ph.D. thesis, California Institute of Technology, 1980 (unpublished); S. Trentalange and C. A. Barnes (unpublished).
[23]M. L. Chatterjee, L. Ptovin, and B. Cujec, Nucl. Phys. **A333**, 273 (1980).
[24]B. Cujec and C. A. Barnes, Nucl. Phys. **A266**, 461 (1976).

[25]P. R. Christensen, Z. E. Switkowski, and R. A. Dayras, Nucl. Phys. **A280**, 189 (1977).
[26]Z. E. Switkowski, R. G. Stokstad, and R. M. Wieland, Nucl. Phys. **A274**, 202 (1976).
[27]B. Dasmahapatra, B. Cujec, and F. Lahlou, Nucl. Phys. **A394**, 301 (1983).
[28]G. Hulke, C. Rolfs, and H. P. Trautvetter, Z. Phys. A **297**, 161 (1980).
[29]S.-C. Wu and C. A. Barnes, Nucl. Phys. **A422**, 373 (1984).
[30]H. Spinka and H. Winkler, Nucl. Phys. **A233**, 456 (1974).
[31]M. Beckerman and C. A. Barnes (private communication).
[32]G. M. Berkowitz, P. Braun-Munzinger, J. S. Karp, R. H. Freifelder, T. R. Renner, and H. R. Wilschut (unpublished).
[33]H. Al-Juwair, R. Ledoux, M. Beckerman, E. Cosman, S. Gazes, M. Salomaa, J. Wiggins, R. Betts, S. Saini, and O. Hansen, Bull. Am. Phys. Soc. **28**, 670 (1983); and (unpublished).